2014

Generation of Sinusoidal Micro-Wrinkles Pattern Using Gradient Grayscale Effect

Xiangxingyu Lin
Lehigh University

Generation of Sinusoidal Micro-Wrinkles Pattern Using Gradient Grayscale Effect

By Xiangxingyu Lin

A Thesis
Presented to the Graduate and Research Committee
of Lehigh University
in Candidacy for the Degree of
Master of Science

In
Department of Mechanical Engineering and Mechanics

Lehigh University

April-2014

Thesis is accepted and approved in partial fulfillment of the requirements for the Master of Science in Department of Mechanical Engineering and Mechanics.

Generation of Sinusoidal Micro-Wrinkles Pattern Using Gradient Grayscale Effect

Xiangxingyu Lin

_____

Date Approved

_____

Thesis Director

_____

(Name of Department Chair)

ACKNOWLEDGMENTS

This thesis is the summary of the research work I did at Lehigh University.

Firstly, I would like to thank my adviser Dr. Yaling Liu for the continuous support of my Master of Science research. His creative ideas and broad knowledge, his hands on experience in manufacturing, and his patience and motivation helped me a lot during the research. Without his logical analysis and strict requirement, this thesis couldn't be finished well enough.

Also, I would say that many thanks to our group mates, Doruk Yunus, Ran He, Wentao Shi. You guys are really joyful and helpful to work with. Besides, I also thanks not limit to Christopher UhI, Salman Sohrabi, Shunqiang Wang with your knowledge in micro-fluid, programming, as well as equipment using guide.

Finally, I would like to thanks to my parents for caring and supporting my studying over these years. And also, I feel really lucky to have my girlfriend--Mengfan's encourage to the M.S thesis writing. I really love you all.

Xiangxingyu Lin

Table of Contents

List of Figures

List of Tables

Abstract

In this thesis, a new digital lithography technology with gradient grayscale level is firstly applied in Micro-wrinkles pattern fabrication. A mathematical model is developed to predict the micro-wrinkles patterns generation through various gradient grey scale effect. By comparing theoretical curing depth and grayscale level versus light intensity, a feasible and logical experiment method is discussed. The sinusoidal waves generated on a surface, i.e. the resolution, wavelength, and amplitude are characterized by optical microscopy and scanning electron microscopy. Results from this study contribute to the fundamental understanding the knowledge on how the grayscale level and surplus growth influence the curing depth on a surface. Meanwhile, the research also contributes to potential applications in optical devices, micro-fluidic device, and cell culture substrates.

Chapter 1. Introduction

1.1 Lithography technology

Since Alois Scenefelder invented the printmaking process of lithography in 1798, lithography technology has been widely developed over these years. Lithography technology can be used to print text as well as artwork onto paper or other suitable materials[1]. Photolithography is also commonly used for fabricating Microelectromechnical systems devices[2-4]. Traditionally, a prepared photo-mask or reticle is used in photolithography process as a master from which the final pattern is derived. Although photolithographic technology is the most commercially advanced form of microlithography, other techniques are also widely used such as electron beam lithography which is capable for higher patterning resolution.

1.1.1 Photomask Lithography

Photomask lithography, also named as optical lithography or photolithography, is a process which micro-fabricate pattern parts of a thin film or the bulk of a substrate. The principle of photolithography is to use light to transfer a geometric pattern from a photomask to a light-sensitive chemical photoresist on the substrate[5]. Then, a series of chemical reaction etches the exposure pattern into, or enables deposition of a new material in the specific pattern upon[6-8]. The basic procedure is shown in Fig. 1.

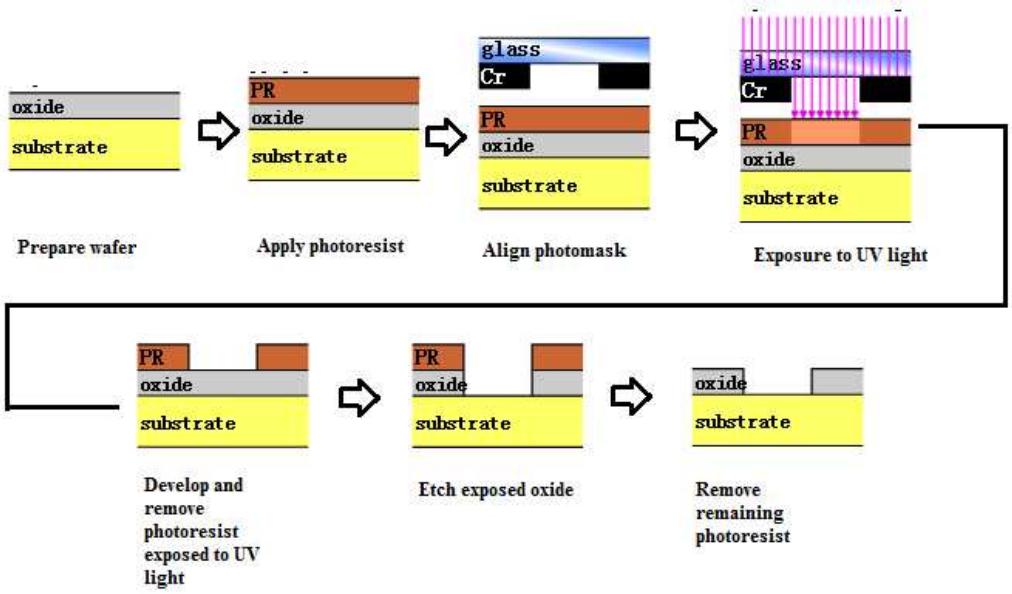

Fig. 1 Photolithgraphy etching process[9]

With pre-heated to a temperature to drive off all moisture that may be present on the surface, the wafer must be chemically cleaned to remove all contamination. Then some adhesion promoters should be applied to promote adhesion of the photoresist to the wafer. The wafer is covered with photoresist by spin coating and prebaked to drive off remaining photoresist solvent. After prebaking, the photoresist is exposed to a pattern of intense light. In etching process, a wet or dry chemical agent removes the uppermost layer of the substrate in the areas that are not protected by photoresist. The finally step is photoresist removal.

1.1.2 Maskless lithography

Another form of lithography is called maskless lithography. The radiation that is used to expose a photoresist is not transmitted through or shot from a photomask. Instead, the radiation is focused to a narrow beam in most cases[10-11]. Then, the beam

directly writes the image onto the photoresist, with one or more pixels at one time. The other method is developed by Micronic Laser Systems or Heidelberg Instruments. It is to scan a programmable reflective photomask, which is then imaged onto the photoresist.

1.2 Grayscale effect definition and its application in lithography

Grayscale pictures are known as a sort of images which are composed by specific level of shade of grey, varying from black at the weakest intensity (grayscale level equals to 0) to white at the strongest intensity (grayscale level equals to 255). Each pixel has its own value which carries only light intensity information. Thus, with the grayscale effect, the light intensity could be controlled during fabrication process. Nowadays, grayscale effect is applied in different areas.

As mentioned in section 1.1, mask photolithography has been widely developed during these years. The traditional lithography is characterized by using the binary exposure method, which means that several areas are exposed under light while other areas remain totally unexposed. Recently, some relatively novel approaches are supposed by grayscale exposure using mask writing technology. The main difference from traditional lithography is that grayscale lithography exposes a gradient of light intensity to photo-resist leading to a potentially much more complicated than its binary counterpart.

Inspired by mask lithography methods, in this thesis, a new method which is combined the grayscale effect with maskless lithography method is proposed.

1.3 Digital maskless lithography

In tradition, maskless lithography always comes with a series of chemical treatments which engraves the exposure pattern into.

In this thesis, a new method that combines maskless lithography with Digital Light Processing (DLP) using the original high intensity light source is developed. The advantage is that the lithography process is simple with shorter pattern generation time, and the surface of printing part can be easily controlled by using this technology.

The process of DLP Photo Maskless Lithography is as follows:

1. Create pattern surface image with dark and bright.
2. Upload the image in the software which can control the exposure time and working area connected with DLP device.
3. Turn on the DLP device with high intensity light source to cure solution on the substrate for tens of milliseconds.
4. Subsequent curing equipment is applied to enforce the curing.
5. Clean the substrate as well as micro-wrinkles pattern with isopropanol solvent.
6. Heat up the micro-wrinkles pattern to remove the remaining solvent.

1.4 Digital Micro-mirror Device in DLP Technology

The Digital Micro-mirror Device is the heart of DLP technology. It is an array of microscopically small, square mirrors-some half a million or more in a small area – each of which can be turned on and off thousands of times per second which allowed images to be projected brighter, sharper and more realistic than has previously been

possible with alternative technologies. Each mirror corresponds to a single pixel in the projected image[12].

A B

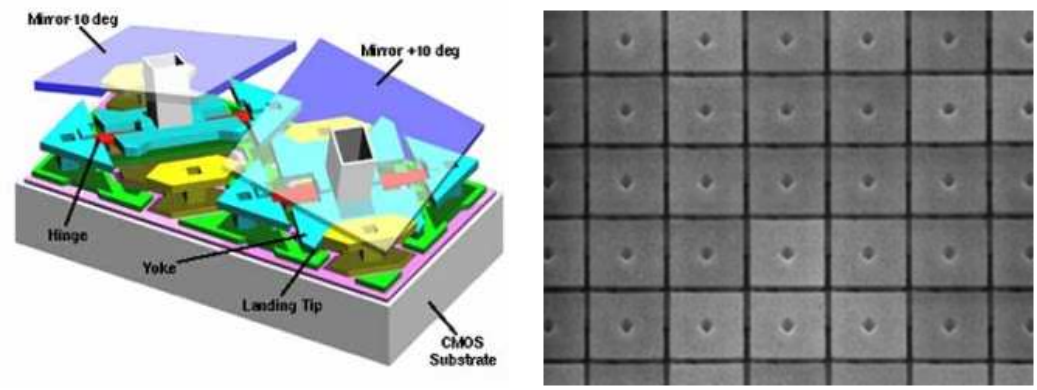

Fig. 2 A. a single micro-mirror with ±10 degree[13]

B. a close-up of the DMD array[14]

With the same structure of DLP, the original light source can be replaced with higher-intensity lamp or Ultra-Violet lamp which can make reaction with photo-curable resin[15-17]. Then, DLP technology is successfully applied in digital lithography technique with minimum resolution of x and y is the size of single pixel in Digital Micro-mirror Device. However, the light will pass through some plastic lens and projection lens after it reflects from Digital Micro-mirror Device. The real best resolution of x and y is much smaller than the size of single pixel in Digital Micro-mirror Device.

The main advantage of DMD-based DLP lithography technology is its high efficiency, since patterns of interest can be generated by only one exposure. Another advantage of DMD-based DLP lithography technology is its surface pattern control. Most of buckling or other spontaneous fabrication methods have no capability to

control its surface pattern. Therefore, if complex custom patterns, such as specific sinusoidal, cosine, sawtooth wave etc., are needed, most of buckling or other spontaneous fabrication methods cannot achieve it. However, DLP lithography has the ability to control its specific surface by changing the grayscale level which is projected or displayed in different areas.

1.5 Introduction of micro-wrinkles pattern

Micro-wrinkle systems have been extensively studied in recent years[18-20]. Micro-wrinkles with micrometer wavelengths have potential utility in various fields such as optical devices, micro-fluidic devices, cell culture substrates and thin film devices, e.g., organic light emitting diodes.

1.5.1 Importance of Micro-wrinkles pattern in various applications

Wrinkles which always exist in rather extended numbers of replicas organized in periodic structure have recently led to the development of various interesting applications. These applications include: pressure sensors, substrates to control the direction of cell growth, substrates to monitor the stress a cell places on a surface, stamps for micro-contact printing, channels with microstructure walls for microfluidic device, diffraction gratings, or functional coatings[21].

It is revealed that the wrinkles enabled the electrode to elongate without appreciable decrease in conductivity and then suggested that when properly engineered, systems comprising thin metal film or glassy conductive polymers

residing on top of elastomeric substrates could be used as interconnects in skin-like flexible electronic circuits.

Another well-known application of wrinkling of rigid films on elastomeric substrates was developed by U.S National Institute of Standards and Technology. A new measurement technique was founded by utilizing wrinkling in thin films to determine the modulus of the skin material[22].

Moreover, researches realized that the micro-wrinkles can be exploited in a range of optical devices, most notably optical gratings. A wrinkles-based diffraction grating was fabricated by Bowden[23].

Micro-wrinkles pattern is also important for microfluidic device research. Channels with micro-wrinkles structure can be used to mimic blood vessels and help capture cells by increasing the chance of cells collision.

1.5.2 Various methods to generate micro-wrinkles pattern

Because of the importance in various applications, micro-wrinkles pattern generation approaches are widely developed during last two decades. The most common way to generate micro-wrinkles pattern is to from micro-wrinkles patterns on hard coating-capped elastomer surfaces spontaneously[24-27]. Typically, they use a thin film which is supported by a relatively soft substrate to fabricate micro-wrinkles. The characteristic of micro-wrinkles, such as the wavelength and amplitude, is determined by the thickness of the hard film and the mechanical properties of the hard film and soft substrate. Four main methods of hard layer formation are widely used[28]:

1. Metals, such as Au, Pt, Ag etc. are directly deposited, onto a soft elastic substrate (Poly dimethylsiloxane PDMS). Spin coating, dip coating, and various plating methods can also be used for the deposition of materials.
2. With mild oxygen plasma treatment, surface modification of silicone rubber can produce the thin film which is also known as hard skin layer.
3. The layer-by-layer method is applied in thin film generation of ionic polymers.
4. Self-supporting thin films, which are prepared separately, can be transferred onto a soft substrate to form heterostructures.

After the preparation step of hard layer, the micro-wrinkles can be formed by the exertion of lateral compressive strain or stress. This step is also known as Buckling-Assisted patterning. There are three main methods for compressive strain field[28].

1. Mechanical force. Compression by a vise.
2. Heat-induced strain method. Thermally-driven compression.
3. Stimuli-driven compression (stimuli sensitive materials).

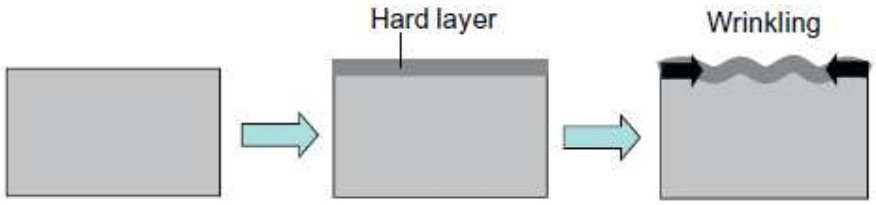

Fig. 3 Mechanism of spontaneous micro-wrinkles pattern generation[28]

Other interesting ways to generate micro-wrinkles pattern were proposed in recent years. Seung Ryong Park, and Seok-Ho song used a light guide plate (LGD) with a two-dimensional array of grating micro-dots to generate micro-wrinkles pattern

on each micro-dot[29]. This method, however, can be classified as photomask lithography way to generate micro-wrinkles pattern. Fig. 4 shows the schematic diagram of a grating micro-dot patterned LGP.

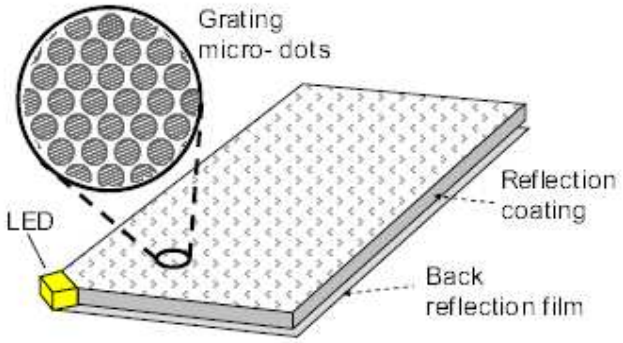

Fig. 4 A schematic diagram of a grating micro-dot patterned LGP used in experiments[29].

Compared with the two traditional ways, DLP technology is firstly applied to micro-wrinkle patterns formation in this thesis, because of its simple fabrication process and practical potential in diverse applications. Another main advantage of applying DLP technology to micro-wrinkle patterns formation is its customized surface pattern. DLP technology can form different specific micro-wrinkle patterns, or make small adjustment for different applications.

1.6 Motivations to use DLP to generate micro-wrinkles pattern

Although there are several methods to generate micro-wrinkles pattern, DLP technology is not limited by only one type of micro-wrinkles pattern. Different shapes of pattern, wavelength, amplitude and combined-shapes can be generated using DLP printing technology. Compared with other methods, DLP has advantages of quicker printing and low cost.

To achieve a better micro-wrinkles pattern, the polymerization characteristic of the solution should be fully understood. The key elements (Light intensity, Photo initiator concentration, Exposure time, Temperature, etc.) which affect curing depth should also be learned in order to achieve precision of micro-wrinkles pattern. Meanwhile, the relationship between grayscale level and light intensity should also be analyzed. In this thesis, theories will be presented and derived in *chapter 2*. Based on these theoretical equation and relationship, experiments are set up to generate different specific parameters of sinusoidal micro-wrinkles patterns. All the experiment equipment and measurement methods are explained in *Chapter 3.* Micro-wrinkles patterns with different wavelengths and amplitude sinusoid are generated. Results and data are analyzed in Chapter 4. Lastly, the conclusion is made and the future work is described.

Chapter 2. Curing process and grayscale effect

2.1 Mechanism of free radical system

In radiation curable systems, Ultra-Violet light which is absorbed by photoinitiator generates free radicals which induce cross-link reactions—mixture of functional oligomers and monomers to generate the cured film. In accordance to free radical mechanism, photo-curable materials cause chain-growth polymerization including three basic steps: initiation, chain propagation and chain termination (shown in table 1). R represents the radical that forms upon interaction with radiation during initiation, and M is a monomer[30]. The active monomer then propagates to create growing polymeric chain radicals. It is worthy to say that propagation step involves reactions of the chain radicals with reactive double bonds of the pre-polymers or oligomers. Generally, the termination reaction usually proceeds through disproportionation, which occurs when an atom (typically hydrogen) is transferred from one radical chain to another resulting in two polymeric chains or through combination, in which two chain radicals are joined together[31].

Initiation
$\mathbf{Initiator + h_\nu \longrightarrow R\bullet}$
$\mathbf{R\bullet + M \longrightarrow RM\bullet}$
Propagation
$\mathbf{RM\bullet + M_n \longrightarrow RM_{n+1}\bullet}$

Termination
Combination
$\mathbf{RM_n\bullet + \bullet M_mR \longrightarrow RM_nM_mR}$
Disproportionation
$\mathbf{RM_n\bullet + \bullet M_mR \longrightarrow RM_n + M_mR}$

Tab. 1 Three basic step of chain-grow polymerization: Initiation, Propagation, Termination[32]

2.2 Theoretical model for curing depth

Over the past decades, two theories have been proposed for curing depth. The first theory came up with the kinetic equations for polymerization[33],

$$-\frac{d[M]}{dt} = R_i + R_p \approx R_p \quad (1)$$

Where

$$R_p = k_p[M][M'] \quad (2)$$

R_p is the polymerization rate, R_i is the free radical initiation rate, [M] is concentration of monomer, [M'] is radical chain concentration, and k_p is a constant for propagation. It is assumed that initiation of radicals equals termination which is also known as steady-state approximation. Thus,

$$R_p = k_p[M]\left(\frac{R_i}{2k_t}\right)^{1/2} \quad (3)$$

Where k_t is a constant for termination. In polymerization process, bi-functional photo initiators are utilized. Then the initiation rate R_i (Einsteins $l^{-3}t^{-1}$) is related to the photonic flux I_z (Einsteins $l^{-2}t^{-1}$) by

$$R_p = 2\phi\epsilon[PI]R_pI_z \quad (4)$$

Where ϕ is the quantum yield of the photoinitiator. ϵ is the molar extinction coefficient ($M^{-1}l^{-1}$), [PI] is the molar concentration of photoinitiator (M), and I_z is

the incident photonic flux at depth z. The photonic flux at depth z is related to the Ultra-Violet intensity at the surface (when z = 0) which follows the Beer's Law:

$$I_z = I_0(10^{-\epsilon[PI]z}) \tag{5}$$

Then equation could be transformed into:

$$R_p = 2\phi\epsilon[PI]R_pI_0(10^{-\epsilon[PI]z}) \tag{6}$$

Plugging equation (6) into equation (3) allows the following expression to be obtained:

$$R_p = k_p[M][\frac{\phi\epsilon I_0[PI](10^{-\epsilon[PI]z})}{k_t}]^{1/2} \approx -\frac{d[M]}{dt} \tag{7}$$

Separating variables and integrating with the assumption of no time dependence in the bracketed term on the RHS, then get following equation:

$$\ln\left(\frac{[M]_0}{[M]}\right) = [\frac{{k_p}^2\phi\epsilon I_0[PI](10^{-\epsilon[PI]z})}{k_t}]^{1/2}t \tag{8}$$

Where $\frac{[M]_0}{[M]}$ on the LHS can be simplified to the degree of polymerization $\bar{x}_n$. $\bar{x}_n$ is also related to the extent of polymerization p as defined,

$$\bar{x}_n = \frac{1}{1-p} \tag{9}$$

At the gel point, $p = p_c$, the critical threshold for gelation. It thus corresponds to limit of the curing depth, z_c, in the photo-curing process and is a characteristic of the photochemical system.

$$\left[\frac{k_t}{{k_p}^2\phi\epsilon I_0}\right][\ln(1-p_c)/t]^2 = [PI](10^{-\epsilon[PI]z_c}) \tag{10}$$

Ultra-Violet light intensity and exposure time are denoted E_{max} in the lithography literature[34]

$$E_{max} = (\frac{chN_{av}}{\lambda})I_0t \tag{11}$$

Where A is the square of lithography part, h is Planck's constant, N_{av} is Avogandro's number, λ is the wavelength of the Ultra-Violet light, c is the speed of

light, and t stands for exposure time.

Substitute equation 11 to equation 10, then the following expression is obtained:

$$\left[\frac{k_t[\ln(1-p_c)]^2 chN_{av}P_L}{{k_p}^2\phi\epsilon\lambda{W_0}^2(2\pi)^{\frac{1}{2}}}\right]\left(\frac{1}{{E_{max}}^2}\right) = [PI](10^{-\epsilon[PI]z_c}) \quad (12)$$

Define variables α^2 (including the photo chemical parameters) as

$$\alpha^2 = \frac{k_t[\ln(1-p_c)]^2}{{k_p}^2\phi\epsilon} \quad (13)$$

β^2 which incorporates the lithography processing parameters.

$$\beta^2 = \frac{chN_{av}P_L}{\lambda{W_0}^2(2\pi)^{\frac{1}{2}}} \quad (14)$$

Substitute equation (13) and equation (14) to equation (12) leads to the following equation:

$$z_c = \frac{2}{2.303\epsilon[PI]}\ln\left(\frac{E_{max}[PI]^{1/2}}{\alpha\beta}\right) \quad (15)$$

The second theory was presented by Jacobs named as standard design equation for lithography as following[35]:

$$C_d = D_p\ln\left(\frac{E_{max}}{E_c}\right) \quad (16)$$

Where C_d means the cure depth, E_{max} presents the energy dosage/area, E_c stands for a critical energy dosage, and D_p is the depth of penetration of the Ultra-Violet light in to resin, which is negative proportional to the molar extinction coefficient and photo-initiator concentration. Analyzing curing characteristic derived from photo-polymerization chemistry, it gives:

$$D_p \Leftrightarrow \frac{2}{2.303\epsilon[PI]} \quad (17)$$

Also E_c is inversely dependent on the photoinitiator concentration to the one-half power as written below:

$$E_c \Leftrightarrow \frac{\alpha\beta}{[PI]^{1/2}} \quad (18)$$

Fig. 5 shows the relation between exposure energy E $(\mathrm{mJ/cm^2})$ and curing depth:

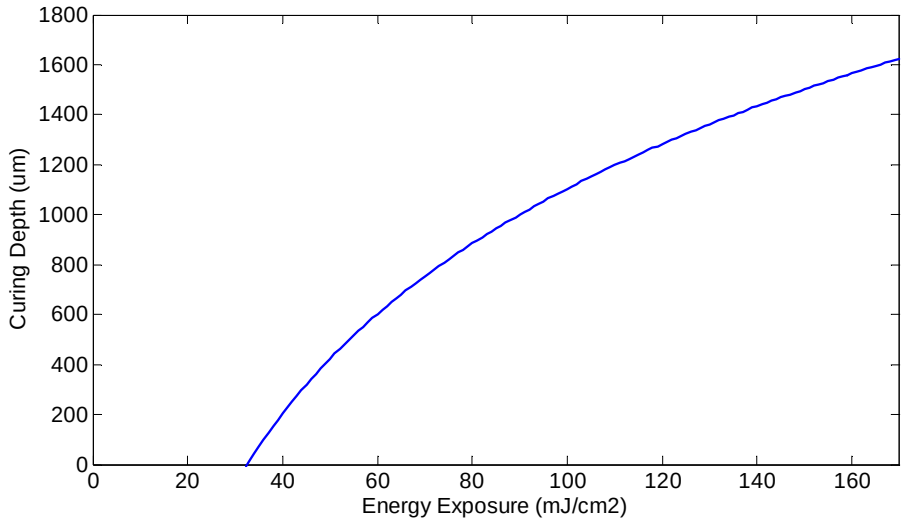

Fig. 5 Energy exposure vs. Curing depth

2.3 Theoretical effect of grayscale

The grayscale digital image is an image which has a certain value for each single pixel. Each value of single pixel carries only intensity information. Images of this sort, also known as black and white, are composed by specific level of grey, varying from black at the weakest intensity (where the value of Grayscale = 0) to white at the strongest (where the value of Grayscale = 255). Figure 6 shows the grayscale distribution from dark (Grayscale level 0) to white (Grayscale level 255). Grayscale images are distinct from one-bit, bi-tonal, black-and-white images, which in the context of computer imaging are images with only the two colors, black, and white (also called bi-level or binary images). Grayscale images have many shades of gray in between. Thus, different values of grayscale are result of different intensity of light at each pixel[36].

Fig. 6 Distribution of grayscale from 0 to 255

With different light intensity exposure in solution, specific pattern can be generated. The exposure intensity is examined by varying the grayscale level. The exposure intensity is normalized by the intensity at a grayscale level of 255 (where is white and intensity is strongest). The exposure intensity is kept almost constant up to a grayscale level of 100. The exposure intensity then exponentially increases with an increase in the grayscale level on the range of 120 to 220. The relationship of grayscale and intensity agrees well with the approximating curve based on the equation (19) as expressed below[37]:

$$I = k_1 \exp(k_2 G_s) \tag{19}$$

Here Gs stands for Grayscale level andk_1, k_2 are constants: $k_1 = 9.2 \times 10^{-3}$, $k_2 = 18.4 \times 10^{-3}$

The following picture shows the relationship between Grayscale level Gs and Light intensity percentage.

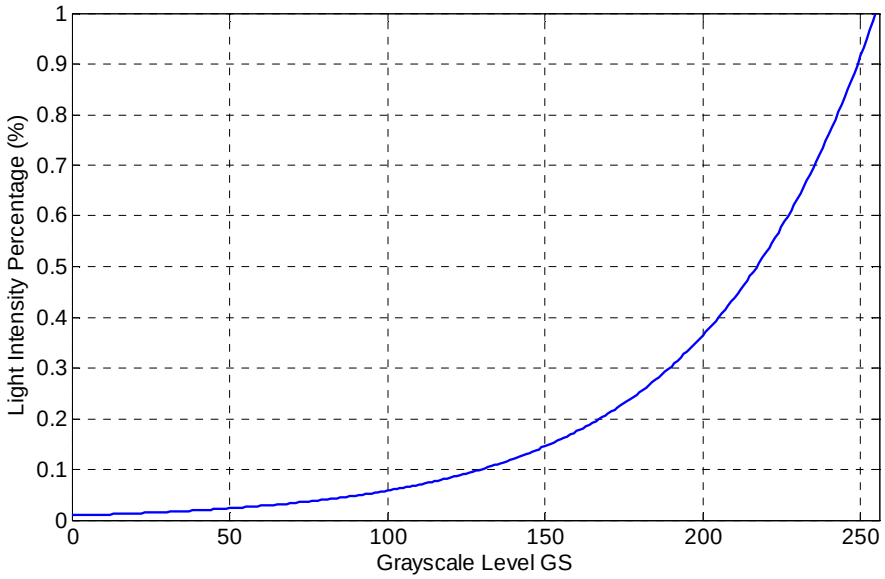

Fig. 7 The relationship between Grayscale level Gs and Light intensity percentage

From the theory of curing depth as well as grayscale effect, it is easy to get the relationship between grayscale level and curing depth, as shown in Fig. 8.

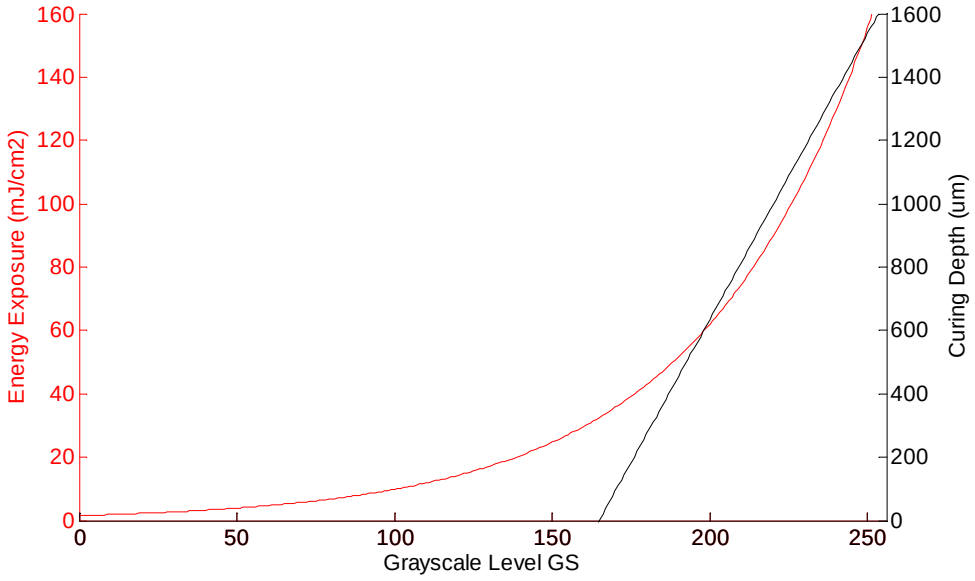

Fig. 8 Relationship between Grayscale level and curing depth

Chapter 3. Experimental setup and materials

The goal of this study is to construct a DLP system that is capable of producing different specific parameters for micro-wrinkles patterns with micrometer scale accuracy.

3.1 Experimental requirements

It is demanding to achieve micrometer details both in horizontal and vertical while manufacturing a micro-wrinkles pattern with precise surface shape. The horizontal resolution depends primarily on the optics. The area of one pixel in Digital Micro-mirror Device determines the minimum unit of micro-wrinkles patterns to achieve best resolution. The vertical resolution, on the other hand, depends mainly on the light intensity, exposure time as well as the resin properties. The exposure time should be optimized to achieve solidification without over-curing. The surface of sinusoidal wave pattern, however, should be precisely controlled by grayscale gradient.

3.2 Selection of solution

As described in Chapter 2, the properties of solution depend on the composition. It can be cured by Ultra-Violet or visible light. Generally the output spectrum of light sources is wide. Solutions, however, tend to have a narrow range of curing spectral for initiation of polymerization. The most efficient design should match the spectra of the light source to the peak wavelength of the polymer.

There are two kinds of polymerization, defined as UVA cured and Visible Light cured[38].

3.2.1 Ultra-violet cured

Many DLP use Mercury Lamps which emit wide spectrum light including Ultra-violet A in the wavelength range between 385 – 400 nm. Polymers initiated below 385 nm are not suitable candidates for DLP lithography since the shorter wavelength Ultra-Violet light rapidly deteriorates the sealants used in most DLP.

3.2.2 Visible Light cured

Light with wavelength range beyond 400 nm is defined as visible light. Polymers initiated above 405 nm are sensitive to light within the visible spectrum. 405 nm is also the wavelength of LED lasers found in Blue Ray drives.

Figure 9 shows the full-wave band spectrum distribution:

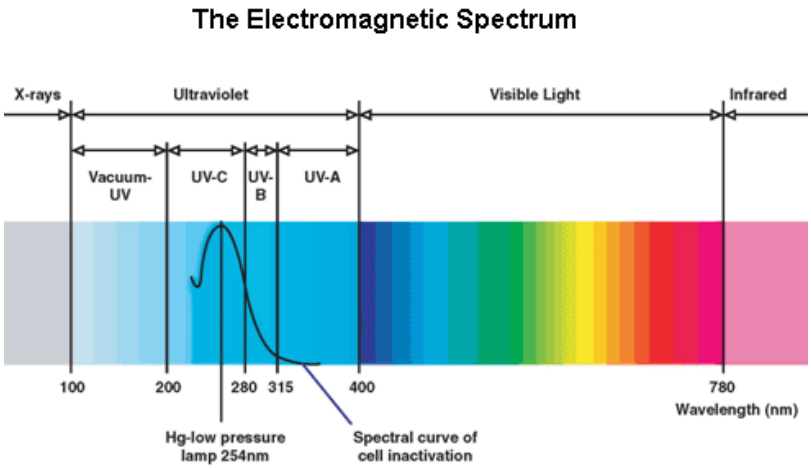

Fig. 9 Full-wave band spectrum[39]

Fig. 9 clearly shows that Ultra-Violet spectrum range from 100 nm to 400 nm, continued with visible light spectrum from 400 nm to 780 nm.

405nm light is mainly absorbed during the printing process. The following table 2 presents the Ultra-Violet wavelength range as well as energy per photon.

Name	Abbreviation	Wavelength Range in Nanometers	Energy per Photon
Ultra-Violet A, long wave	UVA	315nm—400nm	3.10-3.94 eV
Near	NUV	300nm—400nm	3.10-4.13 eV
Ultra-Violet B, medium wave	UVB	280nm—315nm	3.94-4.43 eV
Middle	MUV	200nm—300nm	4.13-6.20 eV
Ultra-Violet c, short wave	UVC	100nm—280nm	4.43-12.4 eV
Far	FUV	122nm—200nm	6.20-10.2 eV

Tab. 2 Ultra-Violet wavelength range and Energy per Photon

In general, the high intensity bulb for DLP is Mercury Vapor Lamp which has full-wave band spectrum.

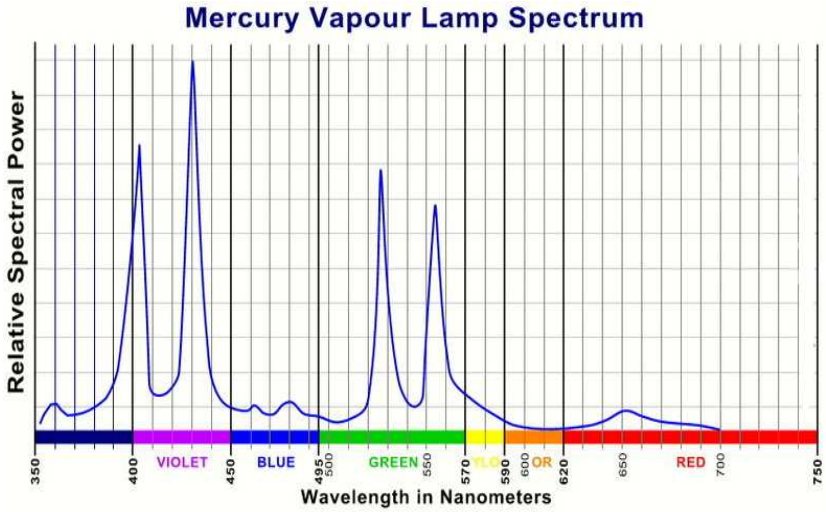

Fig. 10 Typical DLP projector lamp spectrum[40]

Figure 10 shows the typical DLP projector's lamp spectrum. It is obviously that there are two peaks between 400nm—450nm which is around 405nm and 430nm. The

most efficient designs match the spectra of the light source to the peak sensitivity of the polymer. In commercial market for photosensitive resin, there are several kinds of resin whose initiation spectra is around 400 nm—430 nm[41].

In this thesis, MakerJuice G+ green resin is used which can be cured by Ultra-Violet A, B and C light up to around 430 nm. When using Ultra-Violet lasers or high intensity lamps, the cure process is extremely fast. This solution is low odor, zero volatile organic compounds, and only mildly irritant.

3.3 Digital Light Processing apparatus

In this thesis, a bottom-up-based DLP micro-lithography apparatus is constructed for producing micro-wrinkles patterns. This section will look into the equipment composition and the working principles.

Working principles of DLP micro-lithography apparatus are illustrated in following figure 11. Starting from high intensity Mercury Vapor lamp, the light with full-wave band spectrum go through color wheel to change the intensity and wavelength. By passing through different relay lens, light will shoot on the Digital Micro-mirror Device. Meanwhile, millions of micro-mirrors are controlled by computer. Each micro-mirror will change a different small angle which will lead some light paths reflecting to projection lens, whereas other light paths do not reflect to projection lens. In this step, Digital Micro-mirror Device creates the image shown on the computer. It is worthy to mention that the image reflected by Digital Micro-mirror Device has its own limitation depend on the size of pixel in Digital Micro-mirror

Device. By changing the distance of projection lens, smaller image can be obtained. Thus a better (higher) resolution would be obtained by setting up a proper distance of projection lens. Then resin will be cured when the image shoots in the resin. In this thesis, the main purpose is to create micro—wrinkles pattern.

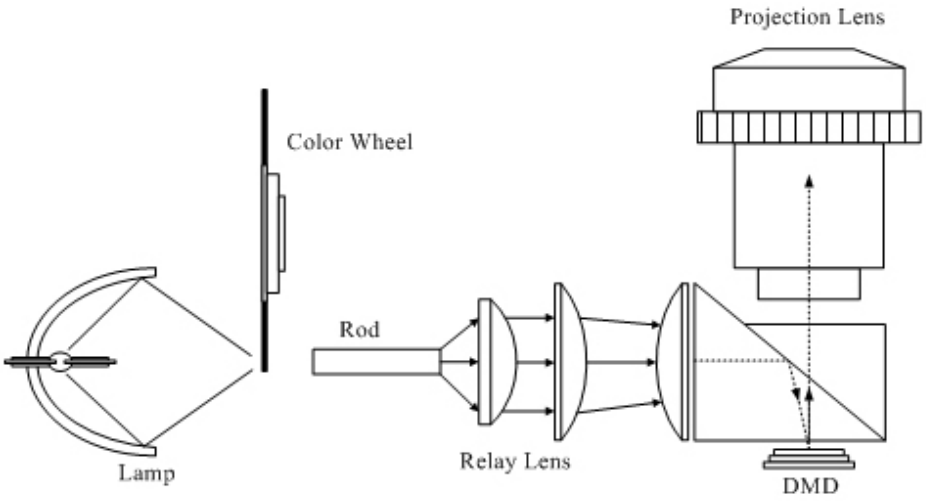

Fig. 11 An illustration of a bottom-up-based DLP micro-lithography apparatus[42]

Considering the limitation of size of a single pixel and light intensity and comparing with different DLP projector, one of the main components in the experiment setup is a commercial video projector Dell 5100MP which is based on DLP technology. The key specifications are shown in table 3:

Dell 5100MP Project Specifications	
Projector Type: Single chip DLP™ DDR	ZOOM: Manual, 1.2X
Brightness: 3300ANSI Lumens(Max)	Bulb Wattage: 300w

Contrast Ratio: 2500:1 (Full on/ Full off)	Power consumption: 400W at full power (335W at Eco-mode)
Resolution: SXGA+ (1400 x 1050)	Power supply: Universal 100-240V AC 50/60 HZ
Deployable Colors: 16.7 Million	I/O Connectors: AC power in, HDMI, RJ-45, VGA (15 pin D-sub), M1, Composite Video, RGB/Component (via DB15), S-Video, RS 232, BNC Connectors, Audio-in and Audio-out ports
Dimensions: 13(W) X 10.3(D) X 4.5(H) inches	Ships with remote control plus power, VGA, S-Video, Composite, RGB Component, 1 Mini pin-to-mini pin and RCA-to-phone jack cables
Image Adjustment: Integrated zoom lens and keystone correction	Standard dedicated support queue and 2 year advance exchange service
Projection distance: 4.92-39.4 feet	Projection screen size: 24.4-292.5'' diagonal(620-7430mm)
Video Compatibility: NTSC, NTSC 4.43, PAL (B/D/G/K/K1/L) and HDTV (480i/P, 576i/P, 720P, 1080i) compatible	Bulb life: 1700hours (Typical)(Up to 2200 hours in Eco-mode)

Tab. 3 Key specification of Dell 5100MP[43]

The structure of Dell 5100MP is shown as below:

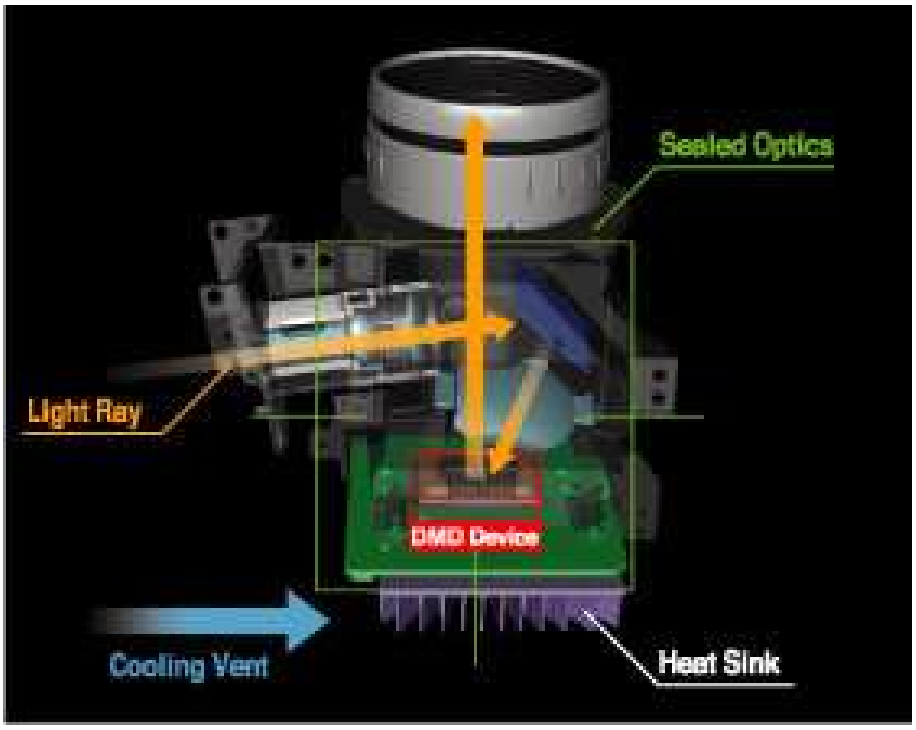

Fig. 12 Dell 5100MP projector optical elements, DMD and projector lens[44]

The original projector lamp is used as the light source. The light is guided through various optical elements inside the projector and finally reflected from the Digital Micro-mirror Device. Dell 5100MP equips with Texas Instruments 0.95 1080p Chipset (Digital Micro-mirror Device) which has the specific parameters shown in the following table 4:

DLP 9500	
Micromirror Array Orientation	Orthogonal
Micromirror Array Size	1920 x 1080
Component Type	DMD
Micromirror Pitch (µm)	10.8
Illumination Wavelength Range (nm)	400-700

Max Display Resolution	1080p

Tab. 4 Parametric for DLP 9500 DMD Chipset[45]

The DMD chip contains 2073600 micromirrors with resolution of 1920 x 1080. Each micromirror corresponds to a single pixel. By turning a single mirror, the pixel in the image is either black or white. Altering the distance of projector lens would break the limitation of size of each pixel. The DLP micro-lithography apparatus is depicted in figure 13. After several experiments (1 in Fig. 14), a certain distance is found to achieve the minimum image with 7.5mm x 9.5mm.

Fig. 13 Inside of Microlithography device with addition distance from lens to DMD

1. Projector lens, 2. Addition distance padding, 3. Light source, 4. Color wheel,

5. Control board, 6. Cooling fan

3.4 Experimental Imaging Software

In this thesis, micro-wrinkles patterns are manufactured and analyzed. To make the method convenient and feasible, the software should give the image of interest. The experiment steps are as followed:

1. Use Matlab to generate specific image with grayscale.
2. Image is presented in PowerPoint with one click dark waiting page and one dark ending page.
3. Set up exposure time in PowerPoint as 1 second.
4. The video projector then is connected to the computer via a VGA cable (15 pin D-sub) and the same grayscale image will be shown in both devices.

3.5 Post-curing equipment

The exposure time should be controlled in 1 second. With the grayscale level around 192, the light intensity is not strong enough to fully cure the resin. It will present as gel status which is needed to add a subsequent curing process. Herein, a Ultra-Violet lamp is used to cure the gel printing part.

3.6 Measurement equipment

The magnitude of sinusoidal micro-wrinkle pattern should be in tens of microns. In order to observe patterns within 100 microns sinusoidal wavelength, Olympus IX70 microscope with 10X objective lens is used. Figure 14 depicts the working process of microscope. Connected to CCD camera, it can directly reflect the image

into computer. Then the wavelength could be measured in pixel unit with translation of 111 pixels equal to 109.6 microns.

Fig. 14 Olympus IX70 acts as measurement equipment

1. Eyepiece, 2. Tungsten Halogen Lamphouse, 3. Apertures, 4. Condenser Lens System, 5. Stage, 6. Fast adjustment and fine adjustment with its self scale mark, 7. Brightness Controller, 8. CCD Camera, 9. Mercury/Xenon Arc Lamp house, 10. Manipulator

Another function of Olympus IX70 is to measure the thickness of each test sample by transferring the scale mark units from sample top side to bottom side to micron units.

In order to observe the cross section of the sinusoidal wave on micro-wrinkles patterns, an electron microscope is also used in the experiment measurement process. Compared with other electron microscope, Hitachi Tabletop Microscope TM-1000 does not need for metal coating preparation. Observation of samples can be carried out quickly with the TM-1000. At the same time, the TM-1000 allows for stereoscopically morphological observation with high resolution and a greater depth of focus which are not available with an optical microscope. The structure of TM-1000 is shown in Fig. 15 as follow.

Items	Description
Magnification	20~10,000X (digital zoom:2, 4X)
Accelerating voltage	15kV
Observation mode	Standard mode/charge-up reduction mode
Specimen traverse	X:15mm, Y:18mm
Maximum sample size	70mm in diameter
Maximum sample thickness	20mm
Electron gun	Pre-centered cartridge filament
Detection system	High-sensitive semiconductor
Frame memory	640 x 480 pixels, 1280 x 960 pixels
Image data memory	HDD of PC and other recording medium
Data display	Micron marker, Micron value,
Evacuation system	Turbomolecular pump: 30L/s x 1 unit
Safety device	Over-current protection function

Tab. 5 Specifications of Hitachi Tabletop Microscope TM-1000

Fig. 15 Hitachi Tabletop Microscope acts as cross-section observation equipment

1. Observation stage, 2. X direction movement, 3. Y direction movement, 4. Exchange button,

5. Electron gun, 6. Control unit, 7 PC, 8. On/Off button.

Chapter 4. Experiments on effect of grayscale level and sinusoidal micro-wrinkles pattern analysis

After introducing the experiments setup and measurement method, in this chapter, Several groups of experiments are set up to find the relationship of grayscale and curing depth as well as the feasibility of sinusoidal micro-wrinkles pattern generation. The later section in this chapter will give an analysis for sinusoidal micro-wrinkles pattern.

4.1 Experiments on the effect of grayscale level

In Chapter 2, theoretical effect of grayscale level has been introduced and in this section an experiment has been set up in order to find out the relationship between grayscale level and curing depth.

Firstly, Matlab code is used to generate different grayscale level separately.

```
Gs=input('Please input the grayscale level= \n')
grayscale=Gs;
image(grayscale);
colormap(gray(256));
```

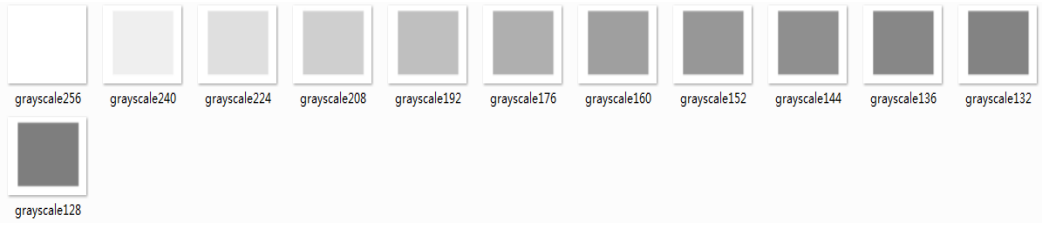

Fig. 16 Matlab generates grayscale from 160-256

Then, using bisection method the minimum grayscale level is found that could cure photo sensitive resin and then the curing depth of each square is recorded. The

experiment steps are followed as below:

1. The half value of 256 is 128. Fit the grayscale 128 in PowerPoint with exposure time 1 second. One waiting page and one ending page should be prepared.
2. Adjust focus point of the projection lens in proper position.
3. Prepare a glass side covered with aluminum foil and fill with solution. The aluminum foil with a little height guaranties the minimum height for solution. Also, the aluminum foil has a square hole in the middle of glass slide for light travelling through.
4. Start PowerPoint and check the status of test square part (cured or not, curing depth, gel or solidification)
5. If the solution isn't cured, upper half value of grayscale (192) should be selected and then the experiment should be repeated.
6. If the solutionis cured, lower half value of grayscale (64) should be selected and then the experiment need to be repeated.
7. Finally, mark the upper side of test square part as well as the upper side of glass side. Then use the Olympus IX70 to measure the thickness of test sample in different grayscale.

Data from several groups of experiments are listed in the following table:

Grayscale level	Calculated value (scale bar)	Total units (scale bar)	Total thickness (μm)	Average thickness (μm)
256	44.3+900	944.3	1605.31	1620.3
	1000-29	971	1650.7	

	44+900	944	1604.8	
240	900-12	888	1509.6	1501.1
	900+8	908	1543.6	
	900-47	853	1450.1	
224	800-30	770	1309	1323.5
	800-14	786	1336.2	
	700+79.5	779.5	1325.15	
208	600+31.5	631.5	1073.55	1078.1
	600+15	615	1045.5	
	600+56	656	1115.2	
192	400-10	390	663	662.2
	400-11	389	661.3	
	400-10.5	389.5	662.15	
176	200-34	166	282.2	287.3
	200-26	174	295.8	
	200-33	167	283.9	
160	NOT CURED			
128	NOT CURED			

Tab. 6 Grayscale level vs. curing thickness experimental data

By using the Olympus IX70 as observation equipment, then the total thickness for each grayscale level is obtained. From Fig. 17, it is obvious that the curing thickness slope turns larger when the grayscale level becomes smaller. It can be inferred that the starting curing grayscale level should be begin with 168 by extending the curve in same slope at grayscale level 176. Fig. 17 shows the relationship between grayscale level and curing depth.

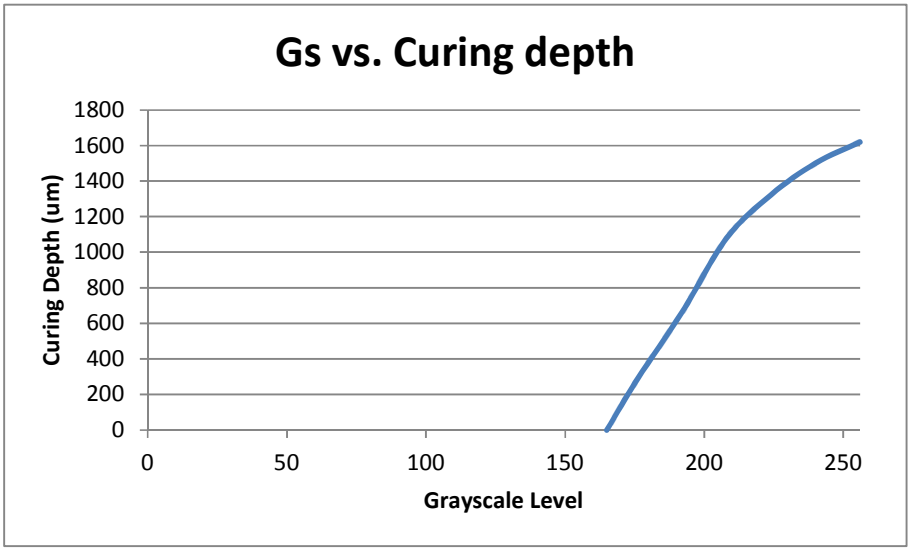

Fig. 17 Relationship between grayscale level and curing depth

In this section, the relationship between grayscale level and curing depth is fully demonstrated by experiments which also meet with theoretical relationship described in Chapter 2 (Figure 8). After understanding the relationship in this specific experiment equipment Dell 5000MP projector, the amplitude of sinusoidal micro-wrinkles pattern can be controlled. The next step is to generate sinusoidal two-dimensional grayscale image in Matlab.

4.2 Using Matlab to generate two dimensional grayscale image

In order to generate sinusoidal grayscale image, the grayscale theory which is demonstrated in Chapter 2 should be understood firstly. Grayscale level is from 1 (black) to 256 (white). The value of sinusoidal wave, however, is from -1 to 1. As it is mentioned before, the largest grayscale level should be in the peak of sinusoidal wave. The same theory is shown that the smallest grayscale level should be in the valley of sinusoidal wave. The grayscale level and the value of sinusoidal wave should follow

the linear equation.

Thus, it is assumed that the highest grayscale level as HG and the lowest grayscale level as LG. The range of sinusoidal wave varies between -1 and 1. In order to rescale sinusoidal wave in grayscale format, the value of sinusoidal wave will match the colormap from LG to HG.

Assume a linear equation for grayscale level and the value of sinusoidal wave as follows,

$$Y = k * X + b$$

Where Y donates the grayscale level and X stands for the value of sinusoid. When X equals to -1 which means the bottom of sinusoid wave, Y should be equal to LG. It is same when X equals to 1 which means the peak of sinusoidal wave, Y should be equal to HG. With these two relationship, factors k and b could be obtained by setting matrix A (coefficient matrix) as [-1 1; 1 1] and matrix B (max and min grayscale level matrix) as [LG; HG]

$$C = \mathrm{inv}(A) * B$$

Where C(1) is the value of k and C(2) is the value of b. Then a two-dimensional grayscale wave image could be generated with the linear equation. Firstly, using the *linspace* function generates linearly spaced vectors. `x=linspace(0,2*pi,1920);` which means that the space from 0 to 2*pi is separated into 1920 sections which is same number of pixel in Digital Micromirror Device. Then the sinusoidal wave function is defined as `sinewave=sin(x*sf);` where sf stands for the number of sinusoidal wave. However, it is one-dimensional sinusoidal wave. In order to transfer

one-dimensional sinusoidal wave into two-dimensional, the following code could transfer one-dimensional sinusoidal wave into two-dimensional matrix.

```
onematrix=ones(size(sinewave));

sinewave2d=(onematrix.*sinewave);
s_sinewave2d=C(1).*(sinewave2d)+C(2);
```

Then two-dimensional grayscale image could be generated directly by using function of *image()* and *colormap(gray(256)).* The full version code is shown in appendix 1.

4.3 Experiment steps for sinusoidal micro-wrinkles generation and Data analysis

In section 4.1, experiments are set up to analyze the factors affecting amplitude of sinusoidal wave – grayscale (or light intensity). The area projected on glass side is 72 square mm which is 7.5 mm in length and 9.6 mm in width. In order to control the wavelength of sinusoidal wave, it is fit in the full projection area and controlled by the number of sinusoidal wave. For example, in order to generate a sinusoidal micro-winkles pattern with wavelength in 150μm, then 64 sinusoidal waves are needed. Thus, the experiments are separated into different groups which are classified by their wavelength. The wavelength and number of sinusoidal wave are as follows:

Wavelength (μm)	2400	1200	600	300	150
Number of sinusoid	4	8	16	32	64
Wavelength (μm)	120	100	80	60	40
Number of sinusoid	80	96	120	160	240

Tab. 7 Different wavelength of sinusoid depends on the number of sinusoid in certain width

With the Matlab program shown in appendix 1, it can generate the two-dimensional sinusoidal grayscale image in different wavelength. In this thesis, the grayscale level from 192 to 256 is researched. The two-dimensional sinusoidal grayscale images are presented as follows.

Fig. 18 Two-dimensional grayscale sinusoidal wave with different wavelength from 40 μm to 2400 μm

The experimental steps for sinusoidal micro-wrinkles pattern are similar to the

previous curing depth test steps:

1. Adjust the focus point of projection lens in proper position.
2. Upload a two-dimensional grayscale sinusoidal wave image with specific wavelength in PowerPoint and set up exposure time as 1 second. One waiting page and one ending page are needed.
3. Prepare a glass side covered with aluminum foil and fill with solution. The aluminum foil with a little height guaranties the minimum height for solution. Also, the aluminum foil has a square hole in the middle of glass slide for light travelling through.
4. Start the PowerPoint and check the sinusoidal micro-wrinkles pattern.
5. Clean the glass side and carefully clean the pattern.
6. Put the pattern into post-curing equipment.
7. Another group of experiment with a different wavelength is setup in PowerPoint and repeats the step 3 to 6.

Repeated experiments for 10 times with different wavelength, 10 groups of sinusoidal micro-wrinkles pattern are obtained. By using Olympus IX70, the following figures show the wavelength of different sinusoidal patterns.

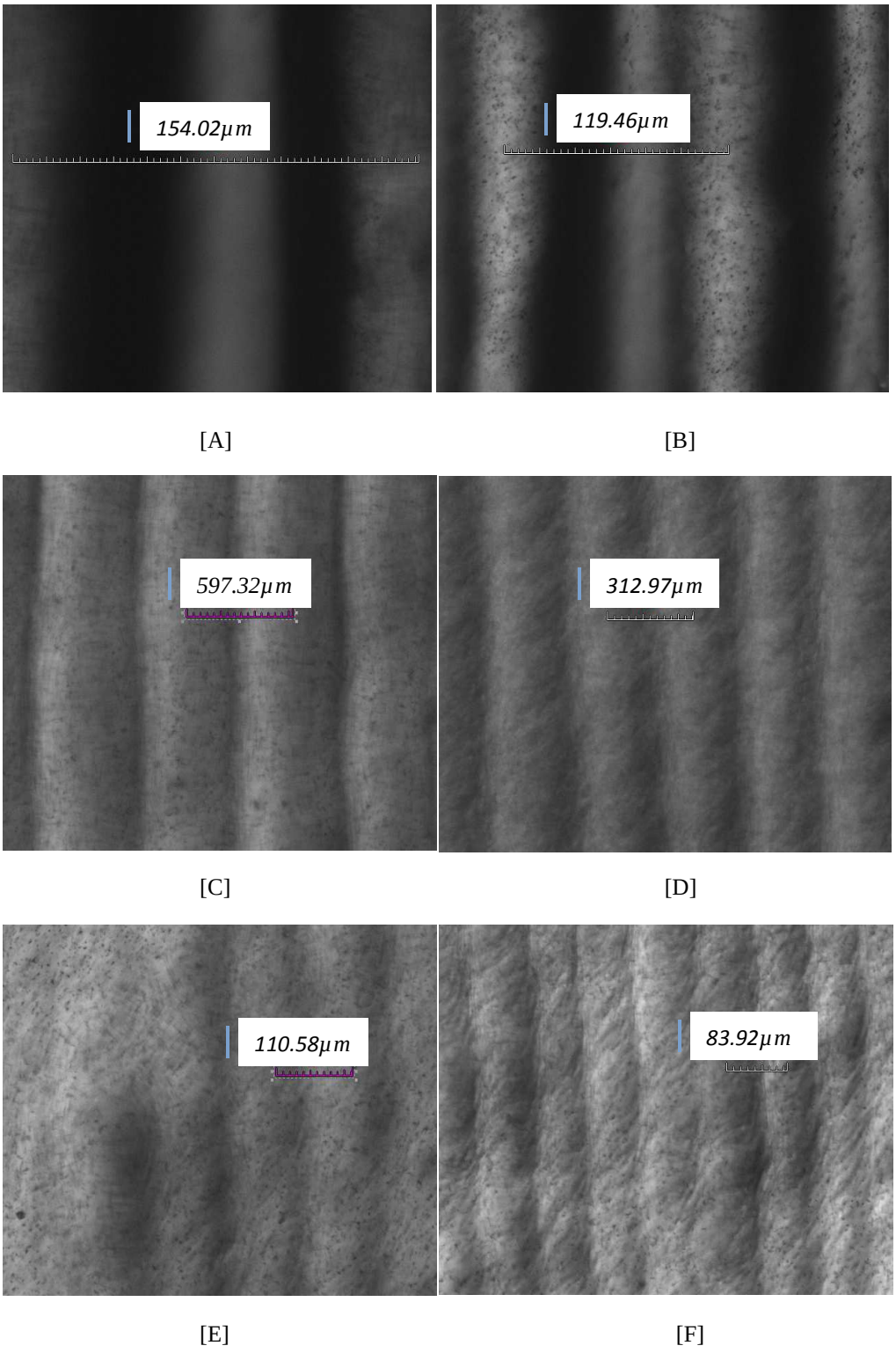

Fig. 19 Micro-wrinkles pattern under Olympus IX70 microscope with different wavelength

A. Optical image of 600 micro wavy pattern, B. Optical image of 300 micro wavy pattern,, C.

Optical image of 150 micro wavy pattern, D. Optical image of 120 micro wavy pattern, E. Optical image of 100 micro wavy pattern, F. Optical image of 80 micro wavy pattern,

Theoretical wavelength (µm)	Actual wavelength (µm)	Error percentage
600	597.3165	0.44%
300	312.9741	4.32%
150	154.0188	2.67%
120	119.4633	0.44%
100	110.5776	10.57%
80	83.9205	4.90%
	Average error percentage	3.89%

Tab. 8 Error percentage in wavelength

Fig. 19 presents six pictures with wavelengths from 80 µm to 600 µm because that wavelength in 1200 µm and 2400 µm is out of range of Olympus IX 70 objective lens. Thus, Fig. 20 is picture taken by a Nikon camera and shows the wavelength in 1200 µm and 2400 µmprofile.

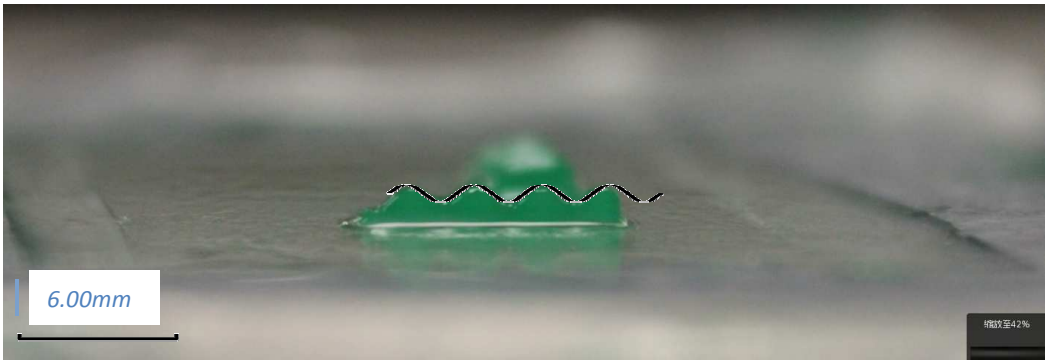

Nikon camera picture captured for wavelength of 2400 µm sinusoidal wave pattern

Black sine wave is the ideal sinusoidal curve

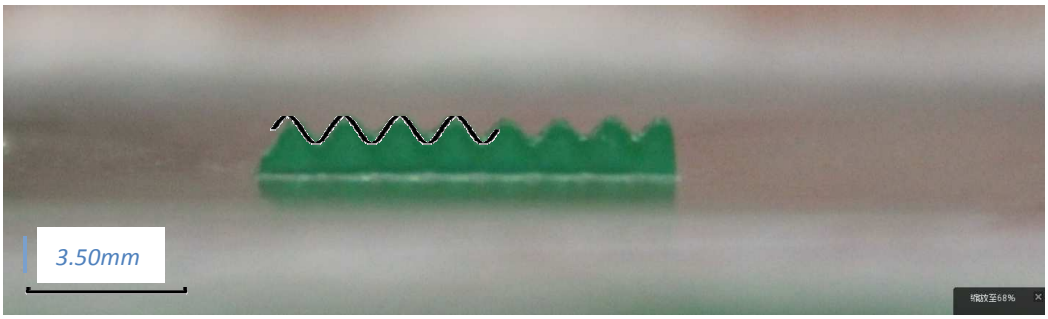

Nikon camera picture captured for wavelength of 1200 µm sinusoidal wave pattern

Black sine wave is the ideal sinusoidal curve

Fig. 20 Nikon camera captured picture for wavelength 1200 µm and 2400 µm

For the wavelength in 60 µm and 40µm, there are no sinusoidal waves shown on the pattern. One possible explanation is that two nearby peaks are too close with a distance of only 4 pixels and 6 pixels because the minimum pixel of Digital Micromirror Device is 10.3 µm. Also, by taking consideration of the surplus growth effect during curing process, there will be no sinusoidal wave shown in pattern. From Fig. 19 and Tab. 8, the error percentage in wavelength is 3.9%.

In order to directly observe the profile of sinusoidal wave on surface as well as the amplitude accurately, the Hitachi Tabletop Microscope TM-1000 is used to observe the surface profile of sinusoidal micro-wrinkles pattern, and then measure the amplitude of sinusoidal wave. The following images show the well formed profile of sinusoidal micro-wrinkles pattern.

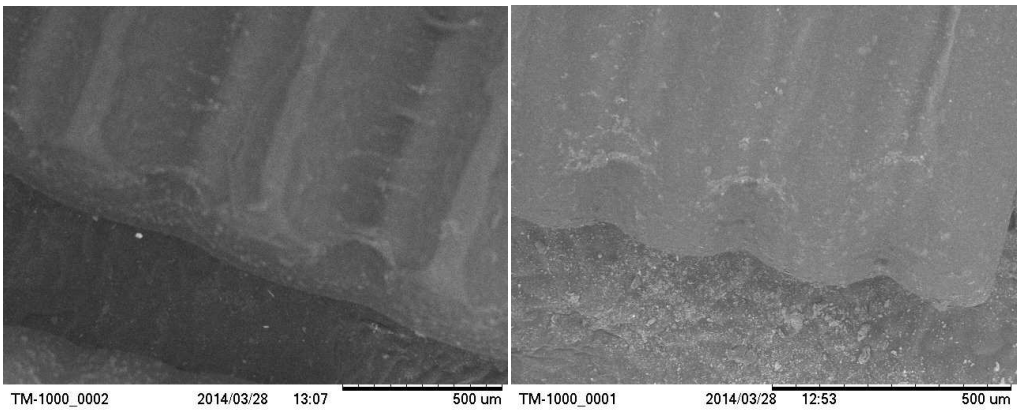

[A] [B]

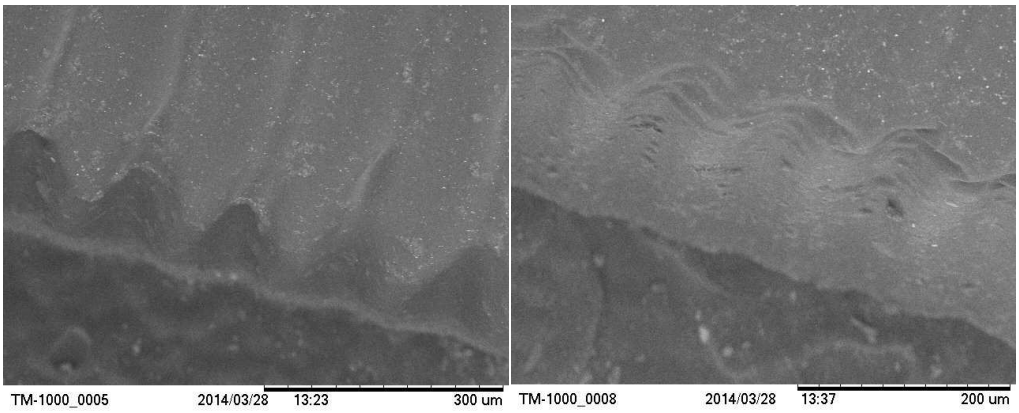

[C] [D]

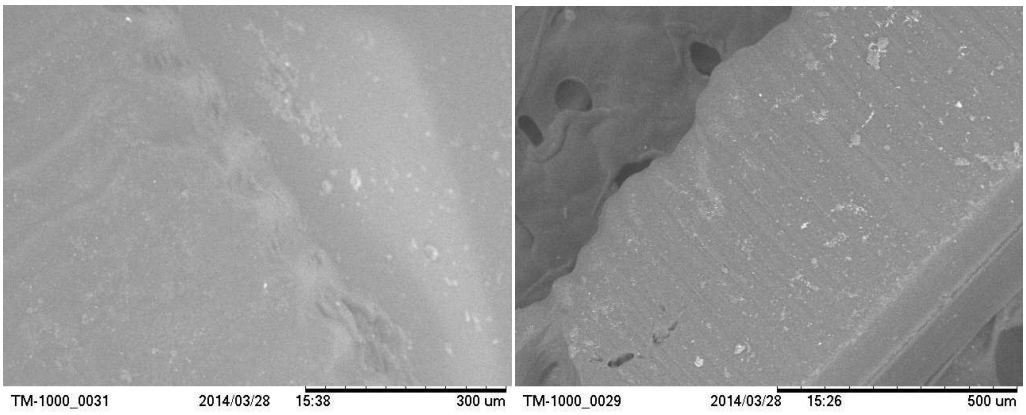

[E] [F]

Fig. 21 SEM images of sinusoidal micro-wrinkles pattern

A. 600 µm sinusoid surface, B. 300 µm sinusoid surface, C. 150 µm sinusoid surface, D. 120 µm sinusoid surface, E. 100 µm sinusoid surface, F. 80 µm sinusoid surface.

From the images captured by Hitachi Tabletop Microscope TM-1000, continuous and smooth sinusoidal wave surfaces are obtained. At the bottom point shown in Fig. 21 [A], it does not show full sinusoidal wave at the bottom because there are some remaining photo sensitive resin and solvent. In order to get a clear observation of sinusoidal wave as well as measurement of amplitude of sinusoidal wave, observation from cross-section is needed. By cutting the micro-wrinkles patterns and observing under the Hitachi Tabletop Microscope TM-1000, the following figures precisely depict the wavelength and amplitude.

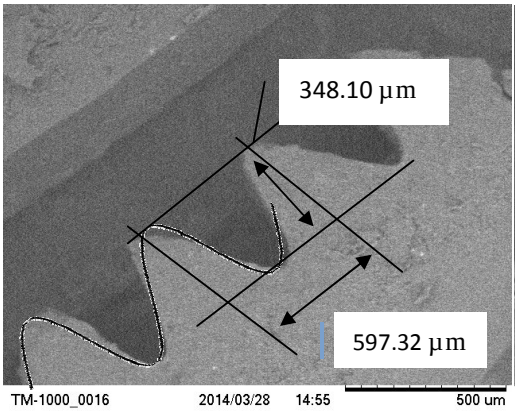

[A]

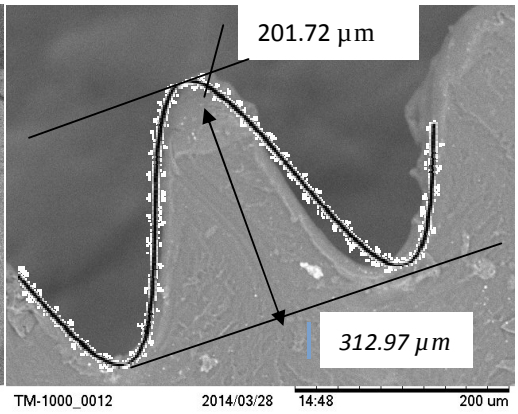

[B]

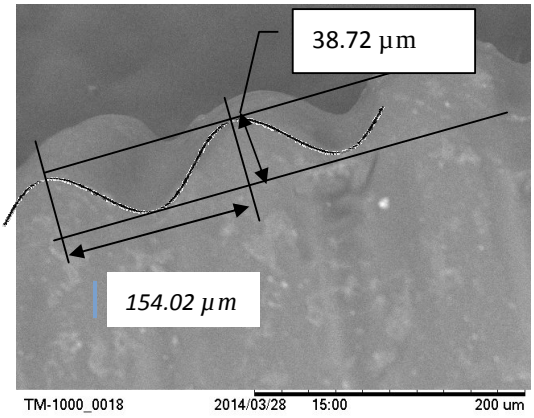

[C]

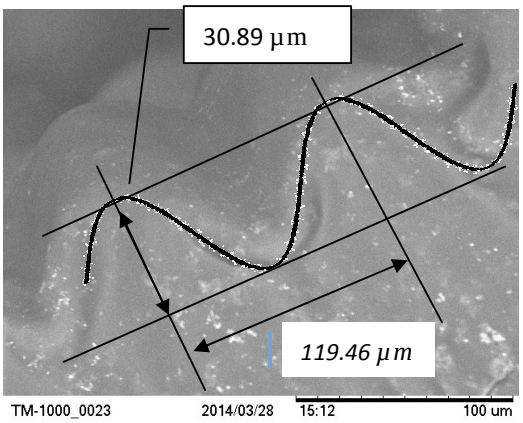

[D]

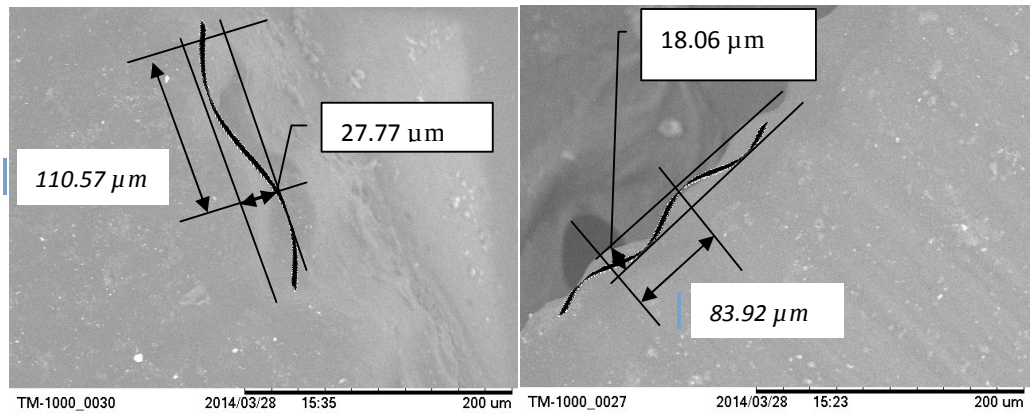

[E] [F]

Fig. 22 Cross-section of sinusoidal micro-wrinkles patterns

A. 600 µm sinusoidal cross-section, B. 300 µm sinusoidal cross-section, C. 150 µm sinusoidal cross-section, D. 120 µm sinusoidal cross-section, E. 100 µm sinusoidal cross-section, F. 80 µm sinusoidal cross-section.

From the cross-section view figures, it is obvious that the amplitude generated in diverse wavelength is quite different.

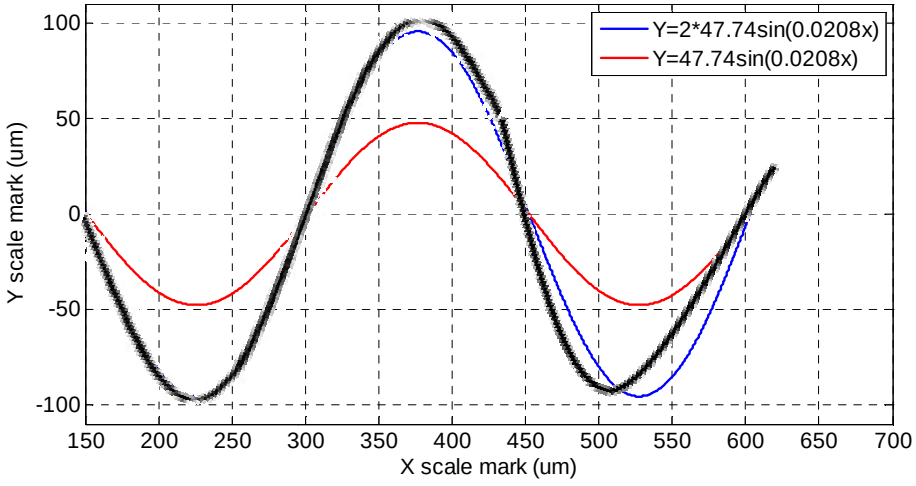

A. Comparison between ideal sinusoid wave and surface profile of patterns (300µm wavelength)

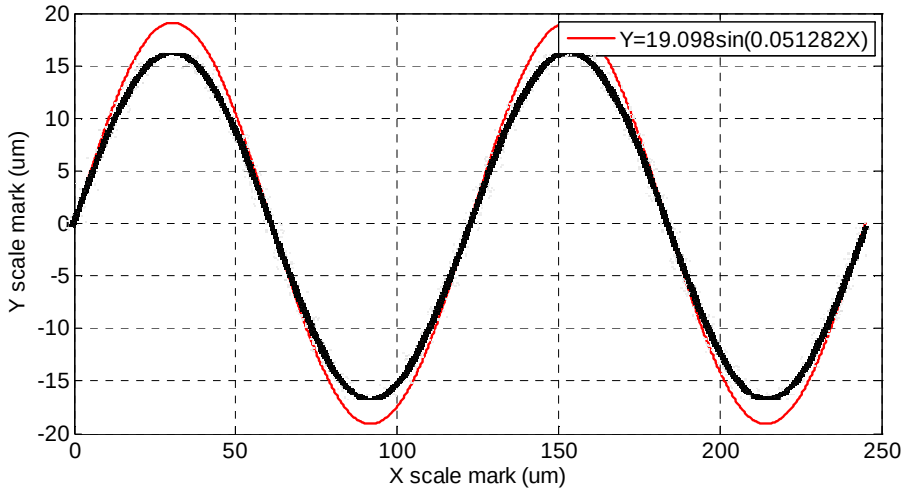

B. Comparison between ideal sinusoid wave and surface profile of patterns (120 μm wavelength)

Fig. 23 Comparison between ideal sinusoid wave and surface profile of patterns

In Fig. 23, the black curve is the captured actual surface profile of generated pattern, the red curve is the ideal sinusoid wave and the blue curve is the ideal sinusoid wave with amplitude doubled (Y=2*sinX). Although all of the patterns are generated under the same grayscale level from 192 to 256 and the same exposure time, the amplitude turns out to be different. Then it can be concluded that the amplitude is not only related with grayscale level and exposure time.

Wavelength (μm)	Amplitude (μm)	Ratio(Amplitude/ Wavelength)
597.32	348.10	0.58
312.97	201.72	0.64
154.02	38.72	0.25
119.46	30.89	0.25
110.57	27.77	0.25
83.92	18.06	0.21
Ideal Sinusoidal Wave Ratio (1/π)		0.32

Tab. 9 Comparison between ideal sinusoid ratio and generated sinusoidal wave pattern ratio

From Tab. 9, it presents that the shorter the wavelength of sinusoid, the smaller ratio is obtained. Compared with ideal sinusoidal wave ratio, it can be inferred that the

surfaces of patterns in 600 μm and 300 μm wavelength have larger amplitude. However, when the wavelength becomes smaller, the ratio becomes smaller which means the surfaces of patterns show an oblate sinusoidal wave. Meanwhile, the height of peak point remains the same value. It means that the height of peak point is related with grayscale level or light intensity and exposure time which follows the relationship shown in Fig. 17. But the amplitude of sinusoidal wave is affected with grayscale level, exposure time and surplus growth effect.

The surplus growth effect can be explained as follow. Suppose the input light energy at a pixel is E (K, t) where K is the light intensity and t is the exposure time. Ideally, the light beam should just cover the inside area of the pixel. Also the light intensity should be uniform inside the pixel shown in figure 24 as pixel α. However, in practice, light from a commercial projector cannot be perfectly focused. Therefore, a light beam of a pixel will spread to its neighboring pixels. Pixel β is a white pixel while pixelχ is a gray pixel with only 0.2 of light intensity of white pixel[46]. Thus, the practical circumstance is depicted in following Fig. 24 as pixel β and pixel χ.

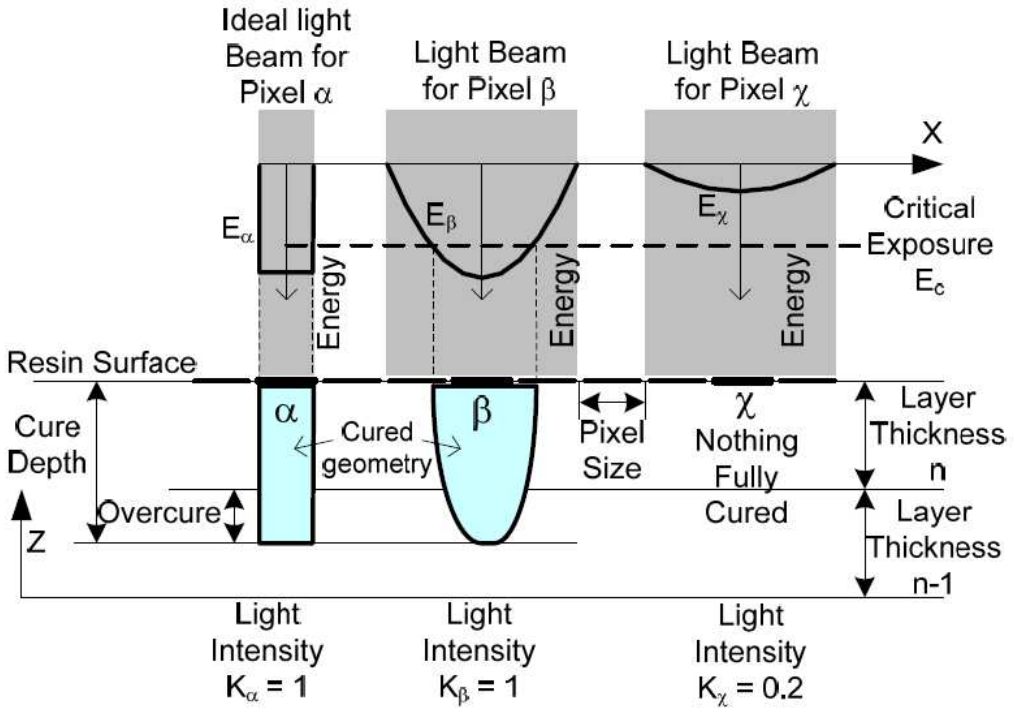

Fig. 24 Principle of surplus growth effect. The light energy of three pixels A, B and C has different shapes and sizes[46]

Thus, affected by surplus growth effect, curing process of each pixel will influence its neighboring pixels curing process. When the wavelength of sinusoidal wave becomes smaller and smaller, the surplus growth effect will be remarkable. Thus, the amplitude of sinusoidal wave is changed.

It is demonstrated that DLP projector is not perfectly focused on a single pixel in the paper by Zhou, Chen and R. Waltz[46]. However, in practice, light beam of each pixel will spread to its neighboring pixels instead referred to the Fig. 24. Also, in this paper, it captures the profile image of each pixel in different grayscale level which is shown as Fig .25. In order to simplify the simulation process, the curing profile is assumed as a parabola equation.

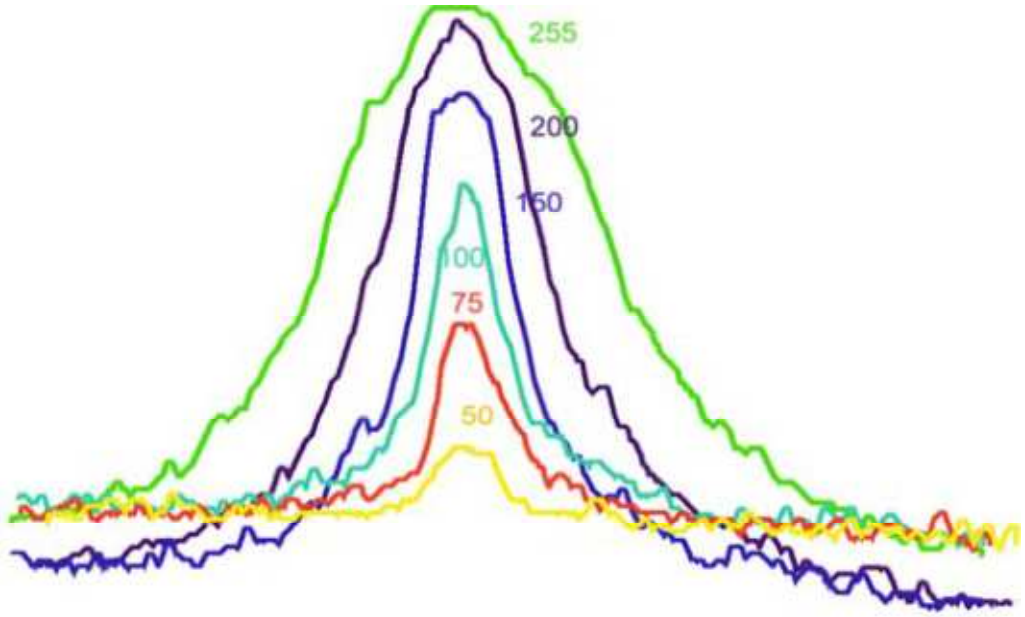

Fig. 25 Light intensity distribution for different grayscale level[46]

Fig. 26 demonstrates the simulation of surplus growth effect. By assuming that the single pixel size is ten microns with surplus growth effect of ten microns, the approximate curing profile follows as parabola function $y = -7.2 * x^2$. The generated parabola functions can be used to simulate the surplus growth effect.

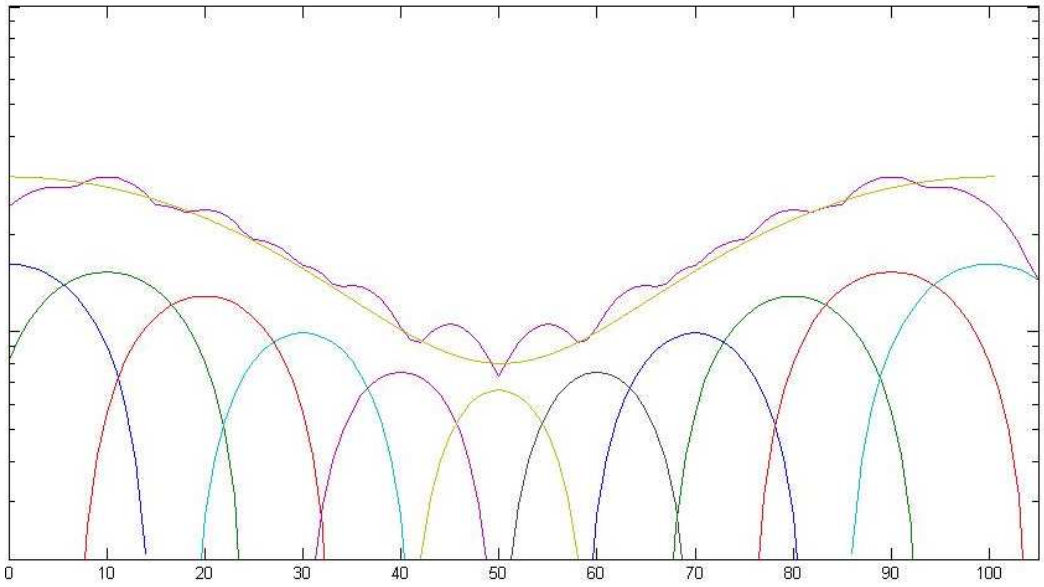

Fig. 26 Simulation of surplus growth effect

In this figure, the bottom parabolas show the simulation profile of cured solution. The upper purple curve shows the surplus growth, while the yellow line shows the ideal cosine wave.

The following table shows the actual amplitude of sinusoidal micro-wrinkles pattern with different wavelength.

Wavelength (μm)	Amplitude (μm)
600	348.10
300	201.72
150	38.72
120	30.89
100	27.77
80	18.06

Tab. 10 Amplitude of sinusoidal micro-wrinkles pattern with different wavelength in grayscale level from 192 to 256

From section 4.1 table 6, theoretical amplitude of sinusoidal wave pattern with grayscale level from 192 to 256 should be 958.12 μm. However, with the effect of surplus growth, the amplitude reduces to 18.06 μm. Thus, it could be concluded that the sinusoidal micro-wrinkles patterns can be generated with amplitude within 50 μm and wavelength between 60 μm to 150 μm.

Chapter 5 Conclusion and future work

In summary, by using the DLP technology, it is feasible to create micro-wrinkles patterns with gradient grayscale. With one second exposure time and grayscale level from 192 to 256, it is possible to generate minimum sinusoidal micro-wrinkles patterns with wavelength of 80 μm and amplitude of 18.06 μm. However, in comparison between actual pattern surface and ideal sinusoidal wave, the micro-wrinkles pattern with wavelength of 120 μm and amplitude of 30.89 μm is more regular and continuous because of the surplus growth effect.

The successful generation of sinusoidal micro-wrinkles patterns by using DLP technology with gradient grayscale means that it is a feasible application in micro-wrinkles patterns generation. With the relationship of grayscale versus curing depth as well as theory of light intensity and effect of surplus growth, the experiment steps mentioned in thesis could be followed by and use DLP method to generate customized surface instead of sinusoidal wave pattern such as square wave, triangle wave, etc. The whole fabrication process is less than one minute which is simple, practical and has potential in diverse applications. It is worthy to mention that its resolution mainly depends on the size of a single pixel, which means that a better resolution would be obtained if the size of pixel in Digital Micromirror Device becomes smaller.

Based on aforementioned discussion, the future work based on this thesis could be extended to micro-wrinkles patterns formation of even smaller scale. By replacing

the DMD with that of higher resolution and smaller pixel size, higher resolution sinusoidal micro-wrinkles patterns with wavelength less than 80 microns could be generated.

Appendix|

Matlab programming code – generate two-dimensional sinusoidal grayscale image:

```
clear all
clc
%%
%get the factor of s_sinewave2d equation
lg=input('please input the lower grayscale= \n');
hg=input('please input the higher grayscale=\n');
A = [-1 1; 1 1];
B = [lg ;hg];
C= inv(A)*B;
%C(1)
%C(2)
%%
%output grayscale wave image
%the total number of pixel should be equal to the last number in bracket
x=linspace(0,2*pi,7);
%sf number of sine
sf=input('please input the number of sine you need: \n');
sinewave=sin(x*sf);
onematrix=ones(size(sinewave));
sinewave2d=(onematrix.*sinewave);
colormap(gray);
imagesc(sinewave2d);
close all
%contrast /* factor of grayscale*/
contrast=1;
s_sinewave2d=C(1).*(contrast.*sinewave2d)+C(2);
image(s_sinewave2d);
colormap(gray(256));
axis off;
```

Appendix II

Matlab code to analyze the relationship between grayscale and curing depth:

```
gs=0:1:255;
i=170*0.0092*exp(0.0184.*gs);
y=982.1352*log(0.030768*170*0.0092*exp(0.0184.*gs));
hl1=line(gs,i,'Color','r');
ax1=gca;
set(ax1,'XColor','r','YColor','r');

ax2=axes('Position',get(ax1,'Position'),'YAxisLocation','right','Colo
r','none','XColor','k','YColor','k');
hl2=line(gs,y,'Color','k','Parent',ax2);
```

Matlab code to simulate the surplus growth effect:

```
x=0:1:105;
y1=max(-7.2012.*x.^2+1620.27,0) ;
y2=max(-7.2012.*(x-10).^2+1528.78,0) ;
y3=max(-7.2012.*(x-20).^2+1289.25,0) ;
y4=max(-7.2012.*(x-30).^2+993.17,0) ;
y5=max(-7.2012.*(x-40).^2+753.64,0) ;
y6=max(-7.2012.*(x-50).^2+662.15,0) ;
y7=max(-7.2012.*(x-60).^2+753.64,0) ;
y8=max(-7.2012.*(x-70).^2+993.17,0) ;
y9=max(-7.2012.*(x-80).^2+1289.25,0) ;
y10=max(-7.2012.*(x-90).^2+1528.78,0) ;
y11=max(-7.2012.*(x-100).^2+1620.27,0) ;
y=y1+y2+y3+y4+y5+y6+y7+y8+y9+y10+y11;
x1=linspace(0,32*pi,50000);
y12=1100*cos(0.0625.*x1)+1900;

plot(x,y1,x,y2,x,y3,x,y4,x,y5,x,y6,x,y7,x,y8,x,y9,x,y10,x,y11,x,y,x1,
y12);
```

Reference

1. Pennel ER, ed. *Lithography and Lithographers.* London: T. Fisher Unwin Publisher (1915).

2. E. F. Reznikova; J.Mohr; H. Hein. *Deep photo-lithography characterization of SU-8 resist layers.* Microsystem Technologies, 2005, **Volume 11**, pp 282-291

3. S.C.H. Thian; Y. Tang; J.Y.H. Fuh; Y.S. Wong; L. Lu; H.T. Loh. *Micro-rapid-prototyping via multi-layered photo-lithography.* Advanced Manufacturing Technology, 2006, **Volume 29**, pp1026-1032.

4. J. Jaczewska; A. Budkowski. *Ordering domains of spin cast blends of conjugated and dielectric polymers on surfaces patterned by soft- and photo-lithogrpahy.* Soft Matter, 2009 , Issue 1, pp 234-241.

5. http://en.wikipedia.org/wiki/Photolithography

6. D. Shir; E.C. Nelson; Y.C. Chen. *Three dimensional silicon photonic crystals fabricated by two photon phase mask lithography.* Applied Physics Letters, **Volume 94**, Issue 1.

7. R. Menon; A. Patel; D. Gil. Maskless lithography. Materials today, 2005, **Volume 8**, Issue 2

8. K.F. Chan; Z. Feng; R. Yang. *High-resolution maskless lithography. Micro/Nanolithography, MEMS , and MOEMS*. **Volume2**, Issue4

9. http://en.wikipedia.org/wiki/File:Photolithography_etching_process.svg

10. R. Menon; A. Patel; D. Gil. Maskless lithography. Materials today, 2005, **Volume 8**, Issue 2

11. K.F. Chan; Z. Feng; R. Yang. *High-resolution maskless lithography. Micro/Nanolithography, MEMS , and MOEMS*. **Volume2**, Issue4

12. Texas Instruments (2013). *Why is the Texas Instruments Digital Micromirror Device so reliable? 2013, From:* http://clifton.mech.northwestern.edu/~me381/papers/intro/ti_micromirror3.pdf

13. Optical Sciences Corporation, http://www.opticalsciences.com/dmd.html

14. Visual Analysis of a Texas Instrument Digital Micro-mirror Dives, http://www.optics.rochester.edu/workgroups/cml/opt307/spr05/john/

15. X. Zhao; C. Zhang. *Digital Manufacturing System Design for Large Area Microstructure Based on DLP Projector*. Journal of Theoretical & Applied Information Technology. 2013 **Vol.48**, Issue 1, P 490-495

16. C. Zhou; Y. Chen. *Calibrating Large-area Mask Projection Stereolithography for Its Accuracy and Resolution Improvements.* 2009, University of Southern California, Los Angeles, CA.

17. G. Frankowski; R. Hainich. *DLP-based 3D metrology by structured light or projected fringe technology for life sciences and industrial metrology*. Emerging Digital Micromirror Device Based systems and Applications. 2009.

18. Kim, H. C; Park, S. M; Hinsberg, W. D. *Block copolymer based nanostructures: materials, processes, and applications to electronics.* Chem, Rev. 2010, **110**, 146-177.

19. de Gennes, P. G; Prost, J. *The physics of Liquid Crystals*, 2nd ed. Oxford University Press: New York, 1993; Chapter 5.

20. Yin, J.; Cao, Z; Li, C.; Sheinman, I.; Chen, X. Stress-driven buckling patterns in spheroidalcore/ shell structures. Proc. Natl. Acad. Sci. U.S.A 2008 **105** 19132-19135

21. Jan, G.; Jan, G. Soft matter with hard skin: *From skin wrinkles to templating and material characterization*. Soft Matter, 2006, advance article on the web.

22. C. M. Stafford, C. Harrison, K. L. Beers, A. Karim, E. J. Amis, M. R. Vanlandingham, H.-C. Kim, W. Volksen, R. D. Miller and E. E. Simonyi, *A buckling-based metrology for measuring the elastic moduli of polymeric thin films, Nat. Mater.* 2004, 3, 545–550.

23. N. Bowden, W. T. S. Huck, K. E. Paul and G. M. Whitesides, *The controlled formation of ordered, sinusoidal structures by plasma oxidation of an elastomeric polymer, Appl. Phys. Lett*, 1999, 75, 2557–2559.

24. Pei-Chun, L.; Shu, Y. *Spontaneous formation of one-dimensional ripples in transit to highly ordered two-dimensional herring hone structures through sequential and unequal biaxial mechanical stretching.* Applied Physics Letters 2007, **90**, 241903.

25. Masashi, W.; Koujirou, M. *Well-Ordered Wrinkling Patterns on Chemically Oxidized Poly(dimethylsiloxane) Surfaces.* Macromolecules 2012, **45**, 7128-7134.

26. Dong-Chun, H.; Geon, M.; Choo, P.; Bong, K.; Younan, X.; Unyong, J. *Buckling-Assisted Patterning of Multiple Polymers.* Advanced Materials 2010,**22**, 2642-2646.

27. Krishnacharya, K.; Junhao, Z.; Shu, Y. *Tunable Open-Channel Microfluidics on Soft Poly(dimethylsiloxane)(PDMS) Substrates with Sinusoidal Grooves.* Langmuir Article 2009 **25(21)**, 12794-12799.

28. Peter A. Fong. *Colloid and Surface Research Trends.* 2007, Published by Nova Science Publisher, Inc, New York **P** 81-82.

29. Seung, P.; Oh, K.; Dongho, S.; Seok-Ho, S. *Grating micro-dot patterned light guide plates for LED backlights.* Optics Express 2007 **Vol. 15**, No.6, 2888.

30. Hoyle, Charles (1990). *Radiation Curing of Polymeric Materials*. Washington, DC: Am. Chem. Soc. pp. 1–15.

31. http://en.wikipedia.org/wiki/Photopolymer

32. Geroge, O. *Principles of Polymerization,* 4th Edition, 2004, A John Wiley & Sons, INC, New York, Chapter 3.

33. Jim, L.; Robert K.; Prude'homme; Ilhan A. *Cure depth in photopolymerization: Experiments and theory,* Materials Research Society 2011, J. Mater. Res., **Vol. 16**, No.12.

34. P.F. Jacobs, *Rapid Prototyping and Manufacturing* (Society of Manufacturing Engineers, Dearborn, MI, 1992).

35. J. H. Lee; R. K. Prud'homme; I. A. Aksay. *Processing of Organic/Inorganic Composites by Stereolithography.* Materials Research Society 2000, Mat. Res. Soc. Symp. Proc., **Vol 625**.

36. Wikipedia; *Grayscale definition.* Wikipedia 2014, From: http://en.wikipedia.org/wiki/Grayscale

37. D. Lee; T. Miyoshi; Y. Takaya; T. Ha; *3D Micro fabrication of Photosesitive Resin Reinforced with Ceramic Nanoparticles Using LCD Microstereolithography.* Journal of Laser Micro/Nanoengineering, 2006 Vol. 1,No. 2 P 142- 148.

38. Lemon, C. *Open Source UV Photopolymer DLP 3D printer*. 2013 Mar 4, From: http://code.google.com/p/lemoncurry/wiki/main

39. UV+IR lamps, http://www.uvir.co.za/UVIRLamps/UVLamps.aspx

40. Open Source UV Photopolymer DLP 3D Printer, https://code.google.com/p/lemoncurry/wiki/main

41. Brain, B. *3D printing: You Want UV Resin?* 2013 October 9, From: http://hackaday.com/2013/10/09/3d-printering-you-want-uv-resin/

42. http://www.ty360.com/2011/5/image/20110503-935-4.jpg

43. http://www.dell.com/downloads/ap/products/brochures/snp/5100mp_projector_brochure.pdf

44. www.sharp-world.com

45. http://www.ti.com/product/dlp9500

46. C. Zhou; Y. Chen, R. A. Waltz. *Optimized Mask Image Projection for Solid Freeform Fabrication.* University of Southern California, Los Angeles, CA

Vita

The author was born in China in 1990. He was awarded bachelor degree with honor in Mechano-electronic engineering in Central South University in Changsha Hu'nan Province in 2012. Following that, he performed research on greyscale effect in Lehigh University. By 2014, he finished his M.S. thesis research.